

Rational Design and Identification of Harmine-Inspired, *N*-Heterocyclic DYRK1A Inhibitors Employing a Functional Genomic *in vivo* Drosophila Model System

Francisco J. Huizar,^c Harrison M. Hill,^a Emily P. Bacher,^a Kaitlyn E. Eckert,^a Eva M. Gulotty,^a Kevin X. Rodriguez,^a Zachary D. Tucker,^a Olaf Wiest,^{*a,b} Jeremiah Zartman,^{*c} and Brandon L. Ashfeld^{*a,b}

^aDepartment of Chemistry and Biochemistry, University of Notre Dame, Notre Dame, IN 46556

^bWarren Family Center for Drug Discovery and Development, University of Notre Dame, Notre Dame, IN 46556

^cDepartment of Chemical and Biological Engineering, University of Notre Dame, Notre Dame, IN 46556

Abstract

Deregulation of dual-specificity tyrosine phosphorylation-regulated kinase 1A (DYRK1A) plays a significant role in developmental brain defects, early-onset neurodegeneration, neuronal cell loss, and dementia. Herein, we report the discovery of three new classes of *N*-heterocyclic DYRK1A inhibitors based on the potent, yet toxic kinase inhibitors, harmine and harmol. An initial *in vitro* evaluation of the small molecule collection assembled revealed that the core heterocyclic motifs benzofuranones, oxindoles, and pyrrolones, showed statistically significant DYRK1A inhibition. Further, the utilization of a low cost, high-throughput functional genomic *in vivo* model system to identify small molecule inhibitors that normalize *DYRK1A* overexpression phenotypes is described. This *in vivo* assay substantiated the *in vitro* results, and the resulting correspondence validates generated classes as architectural motifs that serve as potential DYRK1A inhibitors. Further expansion and analysis of these core compound structures will allow discovery of safe, more effective chemical inhibitors of DYRK1A to ameliorate phenotypes caused by DYRK1A overexpression.

Keywords:

Drug discovery

Biological evaluation

Molecular dynamics simulation

DYRK1A

Molecular scaffolds

High-throughput screen

In vitro/*in vivo* correspondence

Introduction

The dual-specificity tyrosine-phosphorylation-regulated kinase 1A (DYRK1A), is considered an essential kinase in cognitive development and retention.¹⁻⁹ Of the various DYRK isoforms, DYRK1A has received significant attention over the past decade as a potential target for therapeutics development, specifically as it relates to congenital and neurodegenerative cognitive disorders.¹⁰ In contrast to other dual-specificity tyrosine-phosphorylation-regulated kinases (i.e., DYRK1B, DYRK2, DYRK3, and DYRK4),¹¹ *DYRK1A* is ubiquitously expressed and has been implicated in a broad range of disorders.¹²⁻¹⁴ Perhaps most notably, the location of *DYRK1A* in the trisomic region of human

chromosome 21, along with supporting evidence from trisomic mouse models, has led to speculation that the overexpression of *DYRK1A* in individuals affected by Trisomy 21 (Ts21) is at least partially responsible for Down Syndrome (DS)-associated phenotypes.⁷ Developmental alterations in brain morphology due to Ts21 lead to cognitive and behavioral impairments such as memory deficiencies, motor dysfunction, altered synaptic plasticity and early occurrence of (Alzheimer's disease) AD.¹⁵⁻¹⁷ Additionally, the phosphorylation of amyloid precursor protein (APP) and presenilin-1, a component of the γ -secretase complex, by DYRK1A accelerates the generation of neurotoxic A β peptides.¹⁸ Hyperphosphorylation of the microtubule-associated

protein tau by DYRK1A further implicates the overexpression of *DYRK1A* in neurodegeneration.¹⁹

In addition to the aforementioned cognitive disorders, the increase in pancreatic β -cell proliferation upon DYRK1A inhibition implicates DYRK1A as a potential path to treat diabetes.²⁰ Further, recent studies have suggested that because DYRK1A phosphorylates an array of proteins involved in apoptosis, proliferation, cell cycle regulation, and tumor cell senescence, then new chemotherapeutics which modulate DYRK1A activity would be effective anticancer agents.^{21–26} For example, it was shown that *DYRK1A* is overexpressed in glioblastoma, which coincides with DYRK1A-promoted EGFR signal enhancement leading to solid tumor growth.²⁷ These findings suggest that while most of the focus on moderating DYRK1A activity has been toward alleviating cognitive disorders, the development of a potent inhibitor could have far reaching clinical applications across a diverse array of therapeutic areas.

Several designed small molecules and natural products have demonstrated potential as DYRK1A inhibitors, including TG003 ($IC_{50} = 930 \mu M$)²⁸, TBB ($IC_{50} = 4360 nM$)²⁸, GNF2133 ($IC_{50} = 6.2 nM$)²⁹, purvalanol A ($IC_{50} = 300 nM$)²⁸, the β -carboline alkaloid harmine ($IC_{50} = 33 nM$)³⁰, and the polyphenolic green tea extract epigallocatechin gallate (EGCG) ($IC_{50} = 330 nM$)³⁰ (Figure 1).^{31–35} Specifically, these latter two naturally occurring compounds have received significant attention for their inhibitory behavior, and both are hypothesized to competitively bind to the DYRK1A ATP-binding pocket.^{34,36} As with many catechins, EGCG is rapidly metabolized and exhibits poor migratory aptitude across the blood brain barrier (BBB).^{37,38} Thus, although EGCG demonstrates suitable in vitro activity ($IC_{50} = 330 nM$)³⁰, low metabolic stability precludes their use for in vivo phenotypic evaluation of DYRK1A inhibition. In contrast, harmine and its desmethyl analog harmol, are exceptionally potent competitive inhibitors of the DYRK1A ATP-binding pocket ($IC_{50} = 33 nM$)³⁰, but are not routinely used in animal studies because of behavioral side effects associated with monoamine oxidase A inhibition (MOAI) that leads to hallucinogenic effects.^{34,36,38–40} Recently, the azaindole derivative GNF2133 has been shown to exhibit exceptional DYRK1A inhibitory activity ($IC_{50} = 6.2 nM$)²⁹ that appears to enhance β -cell proliferation, a key marker for identifying candidates to treat type I diabetes.²⁹ However, administration of GNF2133 to rat models in vivo induced cellular proliferation in non-targeted tissues such as the liver, heart, and kidney.²⁹ Therefore, while a number of small molecule inhibitors of DYRK1A have been identified, a non-toxic, metabolically stable inhibitor with the potential for kinase selectivity remains elusive. The in

vivo complications associated with small molecules which have shown favorable in vitro DYRK1A inhibition inspired us to embark on a study aimed at the identification of new core scaffolds using a rapid phenotypic in vivo response assay in *Drosophila melanogaster* to probe the impact of exposure to novel compounds. Previous work using *Drosophila* to test novel compounds at the preclinical stages has demonstrated the viability of *Drosophila* as a suitable model organism for therapeutic development.^{41–46}

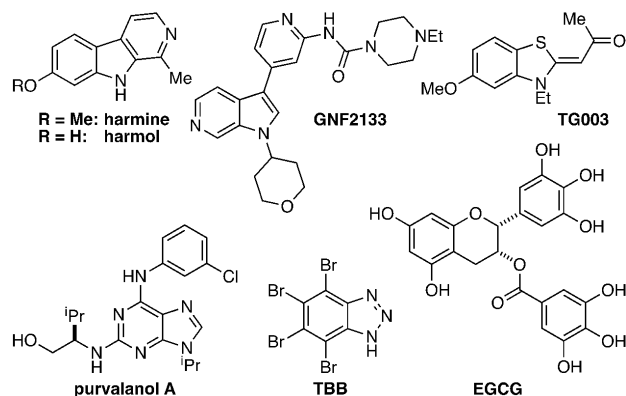


Figure 1. Selected small molecule inhibitors of DYRK1A.

Here, we describe the analysis of the structure-activity relationships of novel DYRK1A inhibitors using in vitro, in vivo, and in silico approaches. Small molecule inhibitors were synthesized by optimizing the attachment groups to six core scaffolds that were designed to have a similar chemical structure to harmine. We report three new classes of *N*-heterocyclic DYRK1A inhibitors, sulfonylated pyrrolones and benzofuranone/oxindole ylides, that successfully inhibit DYRK1A in vivo and in vitro. Furthermore, select compounds demonstrate reciprocal inhibition against recombinant human DYRK1A in vitro, and the *Drosophila* DYRK1A ortholog in vivo. These findings underscore the challenges in reconciling the disparate in vitro and in vivo efficacy of small molecule DYRK1A inhibitors. Further optimization of the identified scaffolds and their associated attachment groups may lead to the identification of a potent, selective DYRK1A inhibitor that can ameliorate disease phenotypes associated with overexpression of DYRK1A.

Results and Discussion

Because the highly conjugated, planar core scaffold present in harmine and harmol is likely a primary cause of the unwelcome promiscuous activity observed, we hypothesized that a non-planar spirooxindole cyclopentenone with spiropyrrolidine **1** bearing H-bond donor/acceptor functionality (blue) would possess comparable inhibitory activity to harmine, and enable the evaluation of phenotypic response in a *Drosophila* model.^{40,47–51} The enhanced 3D topography of the

spirooxindole scaffold has the potential to minimize undesired side effects common among β -carbolines.^{38,39,52–54} The broad spectrum of therapeutic potential, low normal tissue toxicity, and structural properties amenable to BBB penetration of many spirooxindoles prompted us to initiate an exploration of their DYRK1A inhibitory potential as a new chemical probe scaffold in the phenotypic output related to DYRK1A inhibition.^{55–57}

To gain further insight into possible binding modes of harmine and spirooxindole **1** to DYRK1A, we performed molecular modeling studies. Harmine and **1** were first docked to the crystal structure of DYRK1A⁵⁸ (PDB code 2VX3, 2.4 Å resolution) using Glide XP.⁵⁹ These models were then refined by molecular dynamics (MD) simulations (for details, see Supporting Information). Snapshots of the MD simulations of harmine and **1** are shown in Figure 2.

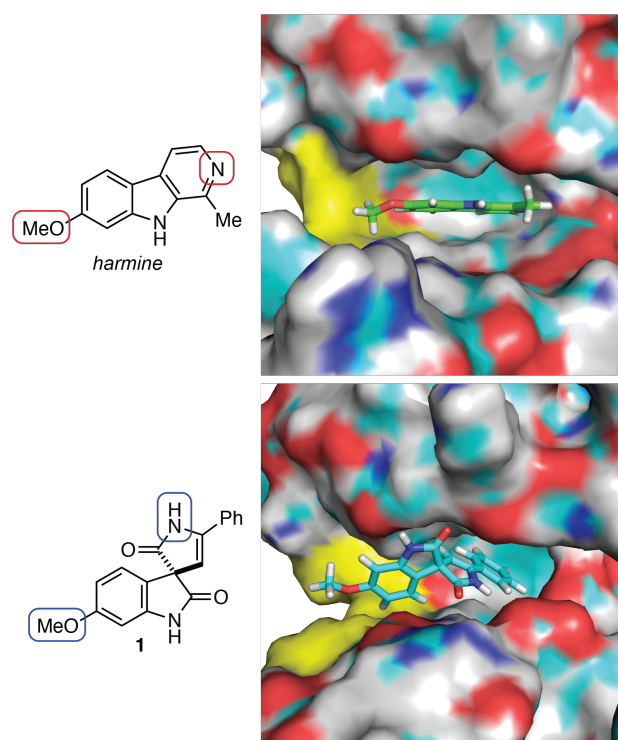


Figure 2. Harmine (top) and spirooxindole (bottom) modeled within the DYRK1A ATP-binding site.

As can be seen, **1** binds very well to DYRK1A. The phenyl ring inserts deeply into the hydrophobic binding pocket formed by A186, V222, F238, L294 and V306. This binding position of the phenyl ring is equivalent to that of the pyridine ring of harmine in DYRK1A. The amide bonds of **1** also form hydrogen bonds with N244 and the backbone of I165. It is noteworthy that the molecular framework of **1** positions the methoxy group closer to the hinge region of the kinase (shown in yellow in Fig. 2), suggesting possibilities for further optimization.

Based on our *in silico* studies of the DYRK1A ATP-binding site with harmine and **1**, we targeted a series of related *N*-heterocyclic substrates and evaluated their efficacy as DYRK1A inhibitors in order to determine the effectiveness of a comparable 3D molecular architecture as a viable DYRK1A active site inhibitor. These docking simulations revealed functionality in harmine and harmol that interact with three primary domains within the ATP-binding pocket of DYRK1A.⁵⁸ Each of the six scaffolds synthesized for this investigation mimic these binding interactions in the kinase hinge region, central domain, and hydrophobic pocket of the active site (Figure 3). The scaffolds investigated include spirooxindole pyrrolones **2**, spirooxindole cyclopentenones **3**, vinyl indolines **4**, sulfonylated pyrrolones **5**, benzofuranone ylides **6**, and oxindole ylides **7** where each scaffold was designed to serve as a molecular probe for DYRK1A inhibition.

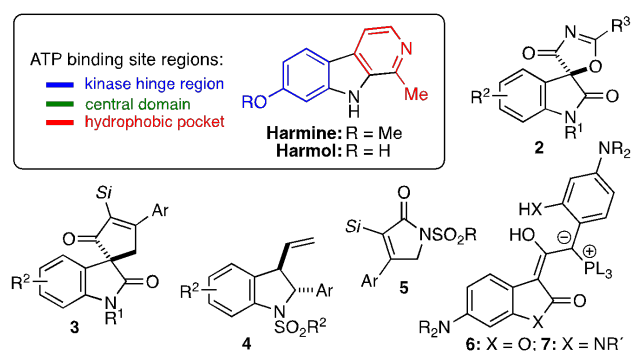


Figure 3. Synthesized novel DYRK1A inhibitors and their predicted DYRK1A ATP-binding site interactions.

We began our study by assembling a collection of spirooxindole oxindoles **2** employing our recently reported (4+1)-cycloadditions of aroyl isocyanates and *in situ* generated oxyphosphonium enolate species.⁶⁰ The oxyphosphonium enolate is generated from the addition of a nucleophilic phosphorous^{III} (i.e., P(NMe₂)₃) to an isatin derivative **8** (Figure 4a). Subsequent addition of an aroyl isocyanate **9**, generated from the corresponding aryl amide and oxalyl chloride, leads to formation of the desired pyrrolone **2** wherein R¹-R³ are readily customized based on the starting materials employed. In a similar fashion, the spirocyclopentenone oxindoles **3** were assembled leveraging our recently reported Rh^{II}-catalyzed (4+1)-cycloaddition between a vinyl ketene, generated *in situ* from an electrocyclic ring opening of the corresponding cyclobutenenone **10**, and a diazooxindole derivative **8**.⁶¹ Initial diazo decomposition followed by cyclopropanation and subsequent ring expansion affords the desired series of substituted spirooxindole cyclopentenones **3** (Figure 4b).

The vinyl indolines **4** were synthesized employing a recently reported Pd^{II}-catalyzed (4+1)-cycloaddition between sulfonyl hydrazones **11** and carbamates **12** (Figure 4c).⁶² The utilization of the well-established

carbamate scaffold afforded access to a diverse array of electron withdrawing and electron donating arene substitution. Likewise, the aryl hydrazone **11** enabled incorporation of various aromatic substituents at the C2-position of the target indoline **4**. Sulfonylated pyrrolones **5** were constructed by a Rh^{II}-catalyzed nitrenoid insertion of sulfonamide **13** into the vinyl ketene derived from cyclobutanone **10** (Figure 4d).

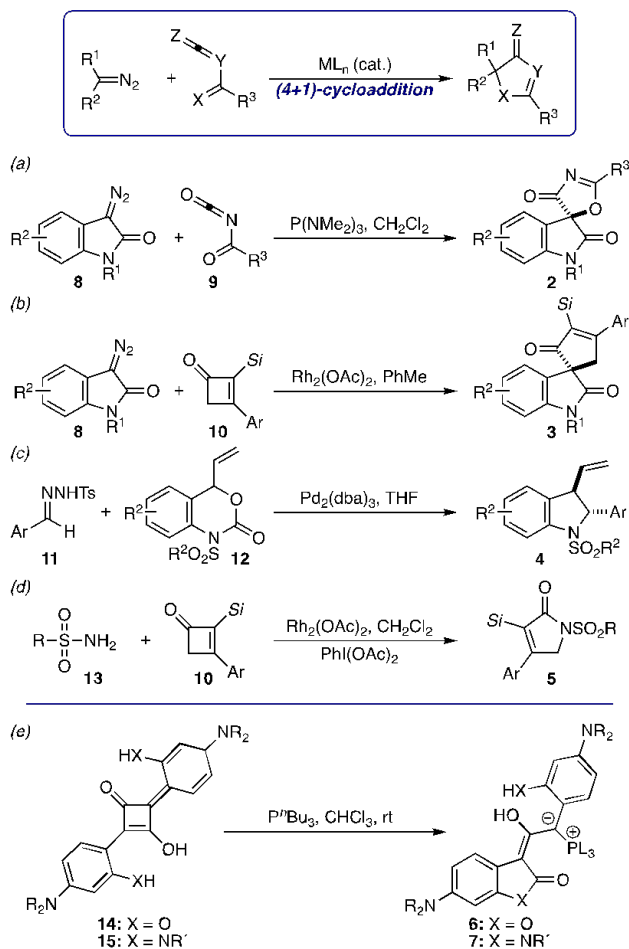


Figure 4. Synthetic approaches to molecular scaffolds of novel DYRK1A inhibitors: (a) phosphorus-mediated cycloannulation of *N*-acyl isocyanates; (b) Rh^{II}-catalyzed cycloaddition of cyclobutenones; (c) Pd⁰-catalyzed assembly of indolines; (d) Rh^{II}-nitrenoid construction of pyrrolones; (e) phosphine-mediated, dearomative rearrangement of dianiline squaraine dyes.

The benzofuranone and oxindole ylides **6** and **7** constitute two of the more exotic architectures evaluated (Figure 4e). During a recent study toward the development of a new class of squaraine dye-based chemodosimeters, we discovered that upon addition of nucleophilic phosphines to ortho-substituted dianiline squaraines, an intriguing dearomative skeletal rearrangement occurred to afford the corresponding enol ylides.⁶³ The extended conjugation exhibited by **6** (X = O) and **7** (X = NR'), where R' is an electron withdrawing functionality that effectively lowers the pK_a of the adjacent N–H, draws comparisons to the β-carboline cores of the potent DYRK1A inhibitors harmine and

harmol. It is notable that benzofuranones **6** and oxindoles **7** are surprisingly stable to a wide array of environmental stimuli and were found to only undergo retroversion to the parent squaraine in the presence of either a strong Brønsted acid or electron deficient transition metal complex. In sum, these synthetic methods provided ready access to a variety of positional and functional group derivatives of each core scaffold targeted for evaluation as novel DYRK1A inhibitors.

With the scaffolds and compound libraries generated, we began our evaluation on the impact of chemical inhibition of DYRK1A activity through an *in vitro* ELISA assay (Figure 5). In the assay, DMSO acted as the negative control and harmine functioned as the positive control. All compounds were screened at a concentration of 10 μM. To determine the activity of each substrate, recombinant human DYRK1A phosphorylation activity was tested. Because DYRK1A phosphorylates dynamin, an antibody for the phosphorylated form of dynamin allowed for a measurable signal (absorbance at 405 nm, OD405) to infer DYRK1A activity.^{64,65} From analysis of the ELISA assay, certain scaffolds showed better kinase inhibitory activity. In particular, the sulfonylated pyrrolones **5** class and the benzofuranone/oxindole ylides **6/7** displayed consistent and statistically significant inhibition of DYRK1A. The spirocyclopentenone oxindoles **2** had promising inhibitory effects for most compounds, but overall exhibited lower levels of activity relative to **5** and **6/7**. While constituents of the spirocyclopentenone oxindole **3** and vinyl indoline **4** classes presented noteworthy inhibitory effects, particularly **3a**, **3b**, **4a**, and **4b**, these classes exhibited variable efficacy. This was demonstrated by analogs displaying no detectable levels of inhibition, such as **3c** and **4c** (SI Figure 1).

Moving forward to an *in vivo* analysis of scaffolds that exhibited promising activity in the ELISA assay, we selected four molecular inhibitors and tested in their ability to rescue an excess growth phenotype induced by DYRK1A/*mbn* overexpression in the adult fruit fly *Drosophila melanogaster* wing. The fruit fly is an established model system for early stage, low-cost *in vivo* testing of drugs.^{42,44–46,66} Further, *Drosophila* have previously been used as a model organism for AD through characterization of APP and Aβ₄₂ transgenic models.^{67–70} The fruit fly has a highly conserved orthologue of DYRK1A called *minibrain* that shares 82% overall protein identity and 91% identity to the ATP-binding sites of DYRK1A.^{71,72} An advantage of *Drosophila*-based disease models is the ability to develop low-cost genetic models of human diseases that provide quantifiable phenotypic readouts.^{73,74} The disease model

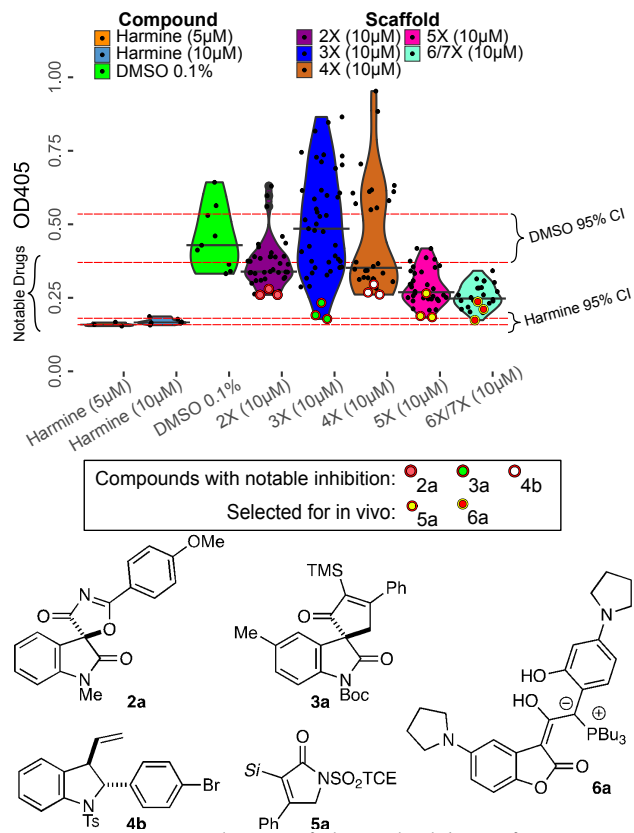


Figure 5. In vitro evaluation of chemical inhibitors for DYRK1A reveals **5** and **6/7** as effective DYRK1A inhibitor scaffolds. Each data point represents a single data point from a 96-well plate absorbance measurement. Each compound was run in triplicate totaling three data points per compound. **5a** (yellow) and **6a** (red) were selected for in vivo testing. **2a** (pink), **3a** (green), and **4b** (white) were notable DYRK1A inhibitors in vitro for other classes.

does not have to correspond directly to the human organ equivalent if there is a clear phenotypic analog connected to the underlying conserved genetic cause.⁷⁵⁻⁷⁷ For example, the thyroid carcinoma therapeutic Vandetanib was identified using *Drosophila* as a disease model although *Drosophila* do not have a thyroid gland.^{43,78} This capability is useful for providing initial, rapid in vivo analysis of new molecules, and has a proven track record for testing novel therapeutics.^{73,74,79} We utilized the GAL4/UAS binary expression system in *Drosophila*⁸⁰ to generate a tissue-specific overexpression model of *DYRK1A/mnb*. Overexpression of *mnb* using the wing specific MS1096-Gal4 driver has previously demonstrated an overgrowth phenotype that can easily be measured.⁷¹ *DYRK1A/mnb* overexpression flies were treated with select synthesized DYRK1A inhibitors to evaluate the efficacy and potency of the inhibitors in vivo (Figure 6).

For the in vivo assay, we tested the kinase inhibitory activity of compounds **5a**, **3d**, **7a**, and **6a**, where the efficacy of each compound was easily evaluated via mounting of the wings and subsequent analysis of their size (Figure 7). Compound leads **5a** and **6a** were selected due to their in vitro efficacy while **3d** was selected due to

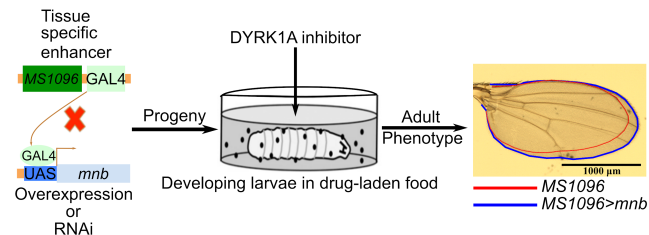


Figure 6. In vivo assay for testing novel DYRK1A inhibitors in *Drosophila melanogaster* with *DYRK1A/mnb* overexpressed in the developing wing primordia. A tissue specific Gal4 driver, MS1096, was used to either overexpress or knock down *DYRK1A/mnb*. Developing larvae were fed synthesized compounds and adult wing areas of males were measured.

its close architectural similarities to the β -carboline harmine and harmol. Likewise, the rather exotic and stable ylide **7a** was selected as a new class of compounds derived from squaraine dyes.⁶³ Thus, we tested two compounds from this class to ensure the viability of the class as a whole in vivo. *Drosophila* exhibiting overexpression were fed with 10 μ M of DMSO or small molecule DYRK1A inhibitors. Overexpression of *mnb* (UAS-*mnb*) significantly increases the wing area of the progeny, while knockdown (UAS-*mnb*^{RNAi}) significantly decreases wing area ($p < 0.001$). Overexpression of *DYRK1A/mnb* in the *Drosophila* wing disc increased adult wing size by 21.36% ($p < 0.001$, Figure 7, SI Table 1). Confidence intervals for wing area medians are overlaid for the overexpression line fed the negative

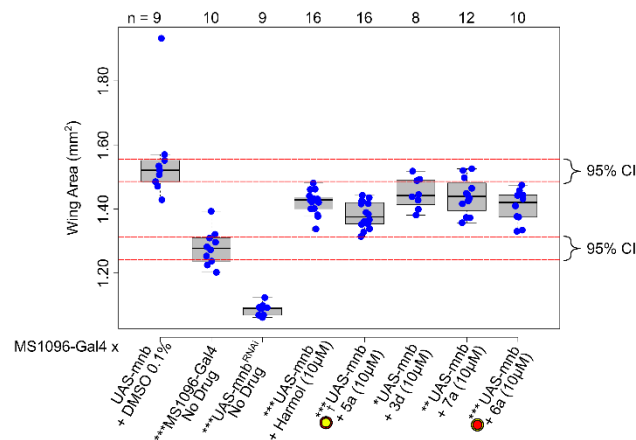


Figure 7. In vivo phenotypic evaluation of DYRK1A inhibitors validates in vitro positive hits by rescuing an overexpression phenotype. **5a** (yellow) and **6a** (red) from the in vitro assay demonstrate statistically significant DYRK1A/*mnb* inhibition. **3d** and **7a** additionally demonstrate statistically significant DYRK1A/*mnb* inhibition. UAS-*mnb* and UAS-*mnb*^{RNAi} indicate *DYRK1A/mnb* overexpression and knockout, respectively. MS1096-Gal4 represents the wing specific transcriptional activator of gene expression. The x-axis demonstrates the genetic cross and the compound fed to developing larvae. Statistical tests were performed using the Mann-Whitney U Test for nonparametric comparison of the effects of tested inhibitors on DYRK1A activity compared to the effects of either DMSO ($p < 0.05$ *, $p < 0.01$ **, $p < 0.001$ ***) or to the effects of harmol ($p < 0.05$ †).

control (DMSO) and for the parental wildtype line with no drugs being administered (red dashed lines). All four of the tested compounds, **5a**, **3d**, **7a**, and **6a**, significantly rescued the overexpression phenotype in comparison to DMSO, with **5a** inhibiting DYRK1A activity to a greater extent than the positive control harmol, a metabolite of harmine (SI Table 1).

Conclusions

In conclusion, we evaluated a small library of compounds deriving from six disparate heterocyclic scaffolds and characterized their impact of chemical inhibition of DYRK1A activity. Of significant importance is the in vitro to in vivo correspondence of compound activity to inhibit DYRK1A for the evaluated compounds. This result is crucial due to other compounds often lacking in vitro to in vivo correspondence in other animal models. To optimize the viability of the identified scaffolds, compound libraries for each scaffold were synthesized with different functional groups attached at specified sites (Figure 4). This serves to improve the selectivity and potency of synthesized DYRK1A inhibitors. This short report paves the way for similar approaches in future studies. While specifically targeting DYRK1A, this study serves as a platform for identification of kinase inhibitors using transgenic *Drosophila* in a low-cost in vivo phenotypic assays. This is transformative to preclinical screening assays of kinase inhibitors to reduce the cost, time, and burden associated with taking a therapeutic from testing to validation. Moreover, the in vivo and in vitro correspondence of tested compounds highlights the potential for the scaffolds to allow discovery of safe, more effective chemical inhibitors of DYRK1A.

ACKNOWLEDGMENTS

The work in this manuscript was supported in part by the National Science Foundation CHE-1956170 (BLA), NIH Grant R35GM124935 (JZ), ND AD&T Discovery Award (JZ, BA), the Leahy-Filipi Fellowship for Excellence in Neuroscience Research (FH), and the Interdisciplinary Interface Training Program Grant (FH), and a CBB Program and NIH training grant T32GM075762 (EPB). We would like to thank the Warren Family Center for Drug Discovery and Dr. John Koren for his contributions in completion of the ELISA assays.

CONFLICT OF INTEREST

The authors declare no conflict of interest.

REFERENCES AND NOTES

1. Neumann, F. *et al.* DYRK1A inhibition and cognitive rescue in a Down syndrome mouse model are induced by new fluoro-DANDY derivatives. *Sci. Rep.* **8**, 2859 (2018).

- Arbones, M. L., Thomazeau, A., Nakano-Kobayashi, A., Hagiwara, M. & Delabar, J. M. DYRK1A and cognition: A lifelong relationship. *Pharmacol. Ther.* **194**, 199–221 (2019).
- Duchon, A. & Herault, Y. DYRK1A, a Dosage-Sensitive Gene Involved in Neurodevelopmental Disorders, Is a Target for Drug Development in Down Syndrome. *Front. Behav. Neurosci.* **10**, (2016).
- Tejedor, F. J. & Hämmerle, B. MNB/DYRK1A as a multiple regulator of neuronal development. *FEBS J.* **278**, 223–235 (2011).
- Lowe, S. A., Usowicz, M. M. & Hodge, J. J. L. Neuronal overexpression of Alzheimer's disease and Down's syndrome associated DYRK1A/minibrain gene alters motor decline, neurodegeneration and synaptic plasticity in *Drosophila*. *Neurobiol. Dis.* **125**, 107–114 (2019).
- Liu, F. *et al.* Overexpression of Dyrk1A contributes to neurofibrillary degeneration in Down syndrome. *FASEB J.* **22**, 3224–3233 (2008).
- García-Cerro, S. *et al.* Overexpression of Dyrk1A Is Implicated in Several Cognitive, Electrophysiological and Neuromorphological Alterations Found in a Mouse Model of Down Syndrome. *PLoS ONE* **9**, (2014).
- Kimura, R. *et al.* The DYRK1A gene, encoded in chromosome 21 Down syndrome critical region, bridges between β -amyloid production and tau phosphorylation in Alzheimer disease. *Hum. Mol. Genet.* **16**, 15–23 (2007).
- Wegiel, J., Gong, C.-X. & Hwang, Y.-W. The role of DYRK1A in neurodegenerative diseases. *FEBS J.* **278**, 236–245 (2011).
- Feki, A. & Hibaoui, Y. DYRK1A Protein, A Promising Therapeutic Target to Improve Cognitive Deficits in Down Syndrome. *Brain Sci.* **8**, (2018).
- Soppa, U. & Becker, W. DYRK protein kinases. *Curr. Biol.* **25**, R488–R489 (2015).
- Arron, J. R. *et al.* NFAT dysregulation by increased dosage of DSCR1 and DYRK1A on chromosome 21. *Nature* **441**, 595–600 (2006).
- Branchi, I. *et al.* Transgenic mouse in vivo library of human Down syndrome critical region 1: association between DYRK1A overexpression, brain development abnormalities, and cell cycle protein alteration. *J. Neuropathol. Exp. Neurol.* **63**, 429–440 (2004).
- Park, J., Song, W.-J. & Chung, K. C. Function and regulation of Dyrk1A: towards understanding Down syndrome. *Cell. Mol. Life Sci.* **66**, 3235–3240 (2009).
- Dierssen, M. Down syndrome: the brain in trisomic mode. *Nat. Rev. Neurosci.* **13**, 844–858 (2012).
- Coppus, A. *et al.* Dementia and mortality in persons with Down's syndrome. *J. Intellect. Disabil. Res.* **50**, 768–777 (2006).
- Becker, L., Mito, T., Takashima, S. & Onodera, K. Growth and development of the brain in Down syndrome. *Prog. Clin. Biol. Res.* **373**, 133–152 (1991).
- Ryu, Y. S. *et al.* Dyrk1A-mediated phosphorylation of Presenilin 1: a functional link between Down syndrome and Alzheimer's disease. *J. Neurochem.* **115**, 574–584 (2010).
- Coutadeur, S. *et al.* A novel DYRK1A (Dual specificity tyrosine phosphorylation-regulated kinase 1A) inhibitor for the treatment of Alzheimer's disease: effect on Tau and amyloid pathologies in vitro. *J. Neurochem.* **133**, 440–451 (2015).
- Dirice, E. *et al.* Inhibition of DYRK1A Stimulates Human β -Cell Proliferation. *Diabetes* **65**, 1660–1671 (2016).
- Hämmerle, B. *et al.* Transient expression of Mnb/Dyrk1a couples cell cycle exit and differentiation of neuronal precursors by inducing p27KIP1 expression and suppressing NOTCH signaling. *Dev. Camb. Engl.* **138**, 2543–2554 (2011).
- Tejedor, F. J. Dyrk1a. in *Encyclopedia of Signaling Molecules* (ed. Choi, S.) 1447–1457 (Springer International Publishing, 2018). doi:10.1007/978-3-319-67199-4_101613.
- Eswaran, J. *et al.* RNA sequencing of cancer reveals novel splicing alterations. *Sci. Rep.* **3**, (2013).

24. Ionescu, A. *et al.* DYRK1A kinase inhibitors with emphasis on cancer. *Mini Rev. Med. Chem.* **12**, 1315–1329 (2012).
25. Abbassi, R., Johns, T. G., Kassiou, M. & Munoz, L. DYRK1A in neurodegeneration and cancer: Molecular basis and clinical implications. *Pharmacol. Ther.* **151**, 87–98 (2015).
26. Guo, X., Williams, J. G., Schug, T. T. & Li, X. DYRK1A and DYRK3 Promote Cell Survival through Phosphorylation and Activation of SIRT1. *J. Biol. Chem.* **285**, 13223–13232 (2010).
27. Pozo, N. *et al.* Inhibition of DYRK1A destabilizes EGFR and reduces EGFR-dependent glioblastoma growth. *J. Clin. Invest.* **123**, 2475–2487 (2013).
28. Becker, W. & Sippl, W. Activation, regulation, and inhibition of DYRK1A. *FEBS J.* **278**, 246–256 (2011).
29. Liu, Y. A. *et al.* Selective DYRK1A Inhibitor for the Treatment of Type 1 Diabetes: Discovery of 6-Azaindole Derivative GNF2133. *J. Med. Chem.* **63**, 2958–2973 (2020).
30. Göckler, N. *et al.* Harmine specifically inhibits protein kinase DYRK1A and interferes with neurite formation. *FEBS J.* **276**, 6324–6337 (2009).
31. Rodriguez, K. X. *et al.* Combined Scaffold Evaluation and Systems-Level Transcriptome-Based Analysis for Accelerated Lead Optimization Reveals Ribosomal Targeting Spirooxindole Cyclopropanes. *ChemMedChem* **14**, 1653–1661 (2019).
32. Muraki, M. *et al.* Manipulation of Alternative Splicing by a Newly Developed Inhibitor of Clks. *J. Biol. Chem.* **279**, 24246–24254 (2004).
33. Mott, B. T. *et al.* Evaluation of substituted 6-arylquinazolin-4-amines as potent and selective inhibitors of cdc2-like kinases (Clk). *Bioorg. Med. Chem. Lett.* **19**, 6700–6705 (2009).
34. Adayev, T., Wegiel, J. & Hwang, Y.-W. Harmine is an ATP-competitive Inhibitor for Dual-Specificity Tyrosine Phosphorylation-Regulated Kinase 1A (Dyrk1A). *Arch. Biochem. Biophys.* **507**, 212–218 (2011).
35. Torre, R. D. la *et al.* Epigallocatechin-3-gallate, a DYRK1A inhibitor, rescues cognitive deficits in Down syndrome mouse models and in humans. *Mol. Nutr. Food Res.* **58**, 278–288 (2014).
36. Jiménez, J., Riverón-Negrete, L., Abdullaev, F., Espinosa-Aguirre, J. & Rodríguez-Arnaiz, R. Cytotoxicity of the β -carboline alkaloids harmine and harmaline in human cell assays in vitro. *Exp. Toxicol. Pathol.* **60**, 381–389 (2008).
37. Abeysekera, I. *et al.* Differential effects of Epigallocatechin-3-gallate containing supplements on correcting skeletal defects in a Down syndrome mouse model. *Mol. Nutr. Food Res.* **60**, 717–726 (2016).
38. Frost, D. *et al.* β -Carboline Compounds, Including Harmine, Inhibit DYRK1A and Tau Phosphorylation at Multiple Alzheimer's Disease-Related Sites. *PLOS ONE* **6**, e19264 (2011).
39. Moloudizargari, M., Mikaili, P., Aghajanshakeri, S., Asghari, M. H. & Shayegh, J. Pharmacological and therapeutic effects of Peganum harmala and its main alkaloids. *Pharmacogn. Rev.* **7**, 199–212 (2013).
40. Rübén, K. *et al.* Selectivity Profiling and Biological Activity of Novel β -Carbolines as Potent and Selective DYRK1 Kinase Inhibitors. *PLoS ONE* **10**, (2015).
41. Sonoshita, M. *et al.* A whole-animal platform to advance a clinical kinase inhibitor into new disease space. *Nat. Chem. Biol.* **14**, 291–298 (2018).
42. Gonzalez, C. *Drosophila melanogaster*: a model and a tool to investigate malignancy and identify new therapeutics. *Nat. Rev. Cancer* **13**, 172–183 (2013).
43. Das, T. K. & Cagan, R. L. A *Drosophila* Approach to Thyroid Cancer Therapeutics. *Drug Discov. Today Technol.* **10**, e65–e71 (2013).
44. Gladstone, M. & Su, T. T. Chemical genetics and drug screening in *Drosophila* cancer models. *J. Genet. Genomics* **38**, 497–504 (2011).
45. Pandey, U. B. & Nichols, C. D. Human Disease Models in *Drosophila melanogaster* and the Role of the Fly in Therapeutic Drug Discovery. *Pharmacol. Rev.* **63**, 411–436 (2011).
46. Viegas Russo Da Conceição Martinho, R. G., De Oliveira Marques, V. M. & Hampson, R. J. Method for Identifying Cancer Drug Candidates in *Drosophila*. (2013).
47. Nathanson, D. & Mischel, P. S. Charting the course across the blood-brain barrier. *J. Clin. Invest.* **121**, 31–33 (2011).
48. Pardridge, W. M. CNS Drug Design Based on Principles of Blood-Brain Barrier Transport. *J. Neurochem.* **70**, 1781–1792 (1998).
49. Cisternino, S., Rousselle, C., Dagenais, C. & Scherrmann, J. M. Screening of multidrug-resistance sensitive drugs by in situ brain perfusion in P-glycoprotein-deficient mice. *Pharm. Res.* **18**, 183–190 (2001).
50. Doan, K. M. M. *et al.* Passive Permeability and P-Glycoprotein-Mediated Efflux Differentiate Central Nervous System (CNS) and Non-CNS Marketed Drugs. *J. Pharmacol. Exp. Ther.* **303**, 1029–1037 (2002).
51. Pardridge, W. M. Drug targeting to the brain. *Pharm. Res.* **24**, 1733–1744 (2007).
52. Gabathuler, R. Approaches to transport therapeutic drugs across the blood-brain barrier to treat brain diseases. *Neurobiol. Dis.* **37**, 48–57 (2010).
53. Ohiri, F. C., Verpoorte, R. & Baerheim Svendsen, A. The African Strychnos species and their alkaloids: a review. *J. Ethnopharmacol.* **9**, 167–223 (1983).
54. De Smet, P. A. G. M. Yohimbe Alkaloids – Corynanthe Species. in *Adverse Effects of Herbal Drugs* (eds. De Smet, P. A. G. M., Keller, K., Hänsel, R. & Chandler, R. F.) 207–209 (Springer, 1997). doi:10.1007/978-3-642-60367-9_17.
55. Miller, K. A. & Williams, R. M. Synthetic approaches to the bicyclo[2.2.2]diazaoctane ring system common to the paraherquamide, stephacidins and related prenylated indole alkaloids. *Chem. Soc. Rev.* **38**, 3160–3174 (2009).
56. Beauchard, A. *et al.* Synthesis of novel 5-substituted indirubins as protein kinases inhibitors. *Bioorg. Med. Chem.* **14**, 6434–6443 (2006).
57. García Prado, E., García Gimenez, M. D., De la Puerta Vázquez, R., Espartero Sánchez, J. L. & Sáenz Rodríguez, M. T. Antiproliferative effects of mitraphylline, a pentacyclic oxindole alkaloid of *Uncaria tomentosa* on human glioma and neuroblastoma cell lines. *Phytomedicine* **14**, 280–284 (2007).
58. Soundararajan, M. *et al.* Structures of Down Syndrome Kinases, DYRKs, Reveal Mechanisms of Kinase Activation and Substrate Recognition. *Struct. England* **1993** **21**, 986–996 (2013).
59. Friesner, R. A. *et al.* Extra Precision Glide: Docking and Scoring Incorporating a Model of Hydrophobic Enclosure for Protein–Ligand Complexes. *J. Med. Chem.* **49**, 6177–6196 (2006).
60. Eckert, K. E. & Ashfeld, B. L. Aroyl Isocyanates as 1,4-Dipoles in a Formal [4 + 1]-Cycloaddition Approach toward Oxazolone Construction. *Org. Lett.* **20**, 2315–2319 (2018).
61. Rodríguez, K. X., Kaltwasser, N., Toni, T. A. & Ashfeld, B. L. Rearrangement of an Intermediate Cyclopropyl Ketene in a RhII-Catalyzed Formal [4 + 1]-Cycloaddition Employing Vinyl Ketenes as 1,4-Dipoles and Donor–Acceptor Metallocarbenes. *Org. Lett.* **19**, 2482–2485 (2017).
62. Tucker, Z. D., Hill, H. M., Smith, A. L. & Ashfeld, B. L. Diverting β -Hydride Elimination of a π -Allyl PdII Carbene Complex for the Assembly of Disubstituted Indolines via a Highly Diastereoselective (4+1)-Cycloaddition. *Org. Lett.* (2020) doi:10.1021/acs.orglett.0c02374.
63. Bacher, E. P. *et al.* A Phosphine-Mediated Dearomative Skeletal Rearrangement of Dianiline Squaraine Dye. *Org. Lett.* (2021).
64. Huang, Y. *et al.* Mnb/Dyrk1A phosphorylation regulates the interaction of dynamin 1 with SH3 domain-containing proteins. *Biochemistry* **43**, 10173–10185 (2004).
65. Liu, Y., Adayev, T. & Hwang, Y.-W. An ELISA DYRK1A non-radioactive kinase assay suitable for the characterization of inhibitors. *F1000Research* **6**, 42 (2017).

66. Botas, J. *Drosophila* researchers focus on human disease. *Nat. Genet.* **39**, 589–589 (2007).
67. Jeon, Y. *et al.* Phenotypic differences between *Drosophila* Alzheimer's disease models expressing human A β 42 in the developing eye and brain. *Anim. Cells Syst.* **21**, 160–168 (2017).
68. Tan, F. H. P. & Azzam, G. *Drosophila melanogaster*: Deciphering Alzheimer's Disease. *Malays. J. Med. Sci. MJMS* **24**, 6–20 (2017).
69. Moloney, A., Sattelle, D. B., Lomas, D. A. & Crowther, D. C. Alzheimer's disease: insights from *Drosophila melanogaster* models. *Trends Biochem. Sci.* **35**, 228–235 (2010).
70. Prüssing, K., Voigt, A. & Schulz, J. B. *Drosophila melanogaster* as a model organism for Alzheimer's disease. *Mol. Neurodegener.* **8**, 35 (2013).
71. Yang, L. *et al.* Minibrain and Wings apart control organ growth and tissue patterning through down-regulation of Capicua. *Proc. Natl. Acad. Sci.* **113**, 10583–10588 (2016).
72. Tejedor, F. *et al.* minibrain: A new protein kinase family involved in postembryonic neurogenesis in *Drosophila*. *Neuron* **14**, 287–301 (1995).
73. Levinson, S. & Cagan, R. L. *Drosophila* Cancer Models Identify Functional Differences Between Ret Fusions. *Cell Rep.* **16**, 3052–3061 (2016).
74. Sonoshita, M. & Cagan, R. L. Chapter Nine - Modeling Human Cancers in *Drosophila*. in *Current Topics in Developmental Biology* (ed. Pick, L.) vol. 121 287–309 (Academic Press, 2017).
75. Hieter, P. & Boycott, K. M. Understanding Rare Disease Pathogenesis: A Grand Challenge for Model Organisms. *Genetics* **198**, 443–445 (2014).
76. McGary, K. L. *et al.* Systematic discovery of nonobvious human disease models through orthologous phenotypes. *Proc. Natl. Acad. Sci.* **107**, 6544–6549 (2010).
77. Shulman, J. M. *Drosophila* and experimental neurology in the post-genomic era. *Exp. Neurol.* **274**, 4–13 (2015).
78. Das, T. & Cagan, R. *Drosophila* as a Novel Therapeutic Discovery Tool for Thyroid Cancer. *Thyroid* **20**, 689–695 (2010).
79. Bangi, E., Murgia, C., Teague, A. G. S., Sansom, O. J. & Cagan, R. L. Functional exploration of colorectal cancer genomes using *Drosophila*. *Nat. Commun.* **7**, 13615 (2016).
80. Duffy, J. B. GAL4 system in *drosophila*: A fly geneticist's swiss army knife. *genesis* **34**, 1–15 (2002).

